

Modelling the dynamical friction timescale of sinking satellite *

Jianling Gan^{1,3}, Xi Kang², Jinliang Hou¹ and Ruixiang Chang¹

¹ Key Laboratory for Research in Galaxies and Cosmology, Shanghai Astronomical Observatory, Chinese Academy of Sciences, 80 Nandan RD, Shanghai, 200030, China

jlgan@shao.ac.cn

² The Purple Mountain Observatory, 2 West Beijing Road, Nanjing 210008, China

³ Graduate School of the Chinese Academy of Sciences, No.19A, Yuquan Rd., 100049 Beijing, China

Received [year] [month] [day]; accepted [year] [month] [day]

Abstract When a satellite galaxy falls into a massive dark matter halo, it suffers the dynamical friction force which drag it into the halo center and finally it merger with the central galaxy. The time interval between entry and merger is called as the dynamical friction timescale (T_{df}). Many studies have been dedicated to derive T_{df} using analytical models or N-body simulations. These studies have obtained qualitative agreements on how T_{df} depends on the orbit parameters, and mass ratio between satellite and host halo. However, there are still disagreements on the accurate form of T_{df} . In this paper, we present a semi-analytical model to predict T_{df} and we focus on interpreting the discrepancies among different studies. We find that the treatment of mass loss from satellite by tidal stripping dominates the behavior of T_{df} . We also identify other model parameters which affect the predicted T_{df} .

Key words: methods: analytical — methods: numerical — galaxies: haloes — galaxies: evolution — galaxies: interactions — cosmology: dark matter

1 INTRODUCTION

In the standard cold dark matter (CDM) model, structure (dark matter halo) grows in a hierarchical manner. During the merger of two dark matter haloes, the less massive one becomes the satellite¹ (or subhalo) of the more massive one (host halo). The satellite will orbit in the host halo and finally merger with the host halo. Halo mergers play an important role in the formation and evolution of galaxies, as they can significantly affect the star formation rate, colors and morphology of galaxies (e.g., Benson et al., 2002, 2004; Kang et al., 2005; Kazantzidis et al., 2008). Therefore, one inevitable question about galaxy formation and evolution in the CDM scenario is to find out how long it takes for the satellite to merge with the host halo.

Dynamical friction is the primary mechanism which decreases the orbital energy and angular momentum of satellite, and drag it to the host halo center. Description of dynamical friction was firstly given by Chandrasekhar (1943), who derived a formula of dynamical friction based on the idealized case that a rigid body moves through an infinite, homogeneous sea of field particles. For most cases, the satellite is moving in a finite host halo, and the dynamical friction timescale (T_{df}) of satellite is defined as the time interval between entry and merger with the host center. The simple application of

* Supported by the National Natural Science Foundation of China.

¹ When we refer satellite, we mean dark matter subhalo, not its luminous part which is often called as satellite galaxy.

Chandrasekhar’s formula to drive T_{df} for a rigid satellite is given by Binney & Tremaine (1987, hereafter BT87) and Lacey & Cole (1993, hereafter LC93), and these formulas are widely used in the semi-analytical models for galaxy formation and evolution (e.g., Kauffmann et al., 1999; Cole et al., 2000; Somerville & Primack, 1999; Neistein & Weinmann, 2010). Early study of Navarro et al. (1995) found that the LC93 formula can accurately match their simulation results. However, the simulation results of Springel et al. (2001) and Kang et al. (2005) have indicated that the LC93 formula underestimates the merging timescale and overestimates the merger rate as LC93 is only valid for a rigid object, not for a living satellite in simulations.

For a live satellite, one needs to take into account the effect of tidal force which leads to the mass loss from satellite and redistribution of mass inside the satellite. Deriving an analytical formula of T_{df} for a live satellite is nontrivial as one has to follow both the orbit and mass evolution. Colpi et al. (1999, hereafter C99) firstly questioned the conclusion of Navarro et al. (1995), and they found that tidal stripping can significantly increase T_{df} . This conclusion was recently confirmed by Boylan-Kolchin et al. (2008, hereafter BK08) and Jiang et al. (2008, hereafter J08) using high resolution simulations. BK08 and J08 both gave fitting formulas for T_{df} , but with different dependence on orbit parameters. Their results differ by a factor up to 2 for eccentric orbits. Using semi-analytical model with the inclusion of tidal effect, Taffoni et al. (2003, hereafter T03) derived a fitting formula for T_{df} . However, their results are not well tested by simulations. Moreover, the prediction of T03 is quantitatively inconsistent with the results of BK08 and J08.

In this paper, we use a semi-analytical model to study T_{df} of satellite. Our main motivation is neither to get a consistent result with simulation or other models, nor to derive a reasonable T_{df} , but to see how the model predictions are affected by various physical processes. This will tell us which process dominates the predicted T_{df} , and how to interpret the discrepancies among the previous studies. Our model is based on Taylor & Babul (2001) and Zentner & Bullock (2003), but with a few modifications. The paper is organized as follows. In Section 2 we review the previous results. We introduce our model in Section 3, and compare our model predictions with the previous work in Section 4, and we summarize and conclude briefly in Section 5.

2 THE PREVIOUS RESULTS

2.1 Set Up of Initial Conditions

The first step of modelling the evolution of satellite is to set its initial conditions, including the orbit energy, angular momentum and initial position. The satellite is assumed to start its orbit at the virial radius, R_{vir} , of the host halo. It has an initial orbital energy equal to that of a circular orbit of radius ηR_{vir} , and the initial specific angular momentum of satellite is parameterized as $j(0) = \varepsilon j_c$, where j_c is the specific angular momentum of the circular orbit mentioned above and ε is the orbital circularity (note that $0 \leq \varepsilon \leq 1$). In the following, we use R_m to denote the initial mass ratio between the host and satellite halo, i.e., $R_m = M_h(0)/M_s(0)$.

2.2 The Previous Results

Here we briefly review the previous studies on T_{df} from analytical models or N-body simulations. Using the Chandrasekhar’s formula, BT87 derived an expression of T_{df} for satellite starting with circular orbit in an isothermal distributed host halo as

$$T_{\text{df,BT87}} = \frac{1.17}{\ln \Lambda} R_m \tau_{\text{dyn}} \quad (1)$$

where τ_{dyn} is the dynamical time $R_{\text{vir}}/V_{\text{vir}}$, and $\ln \Lambda$ is the Coulomb logarithm.

Taking into account the dependence on the orbital circularity, LC93 obtained that

$$T_{\text{df,LC93}} = \frac{\varepsilon^{0.78}}{0.855} \frac{R_m}{\ln \Lambda} \eta^2 \tau_{\text{dyn}}, \quad (2)$$

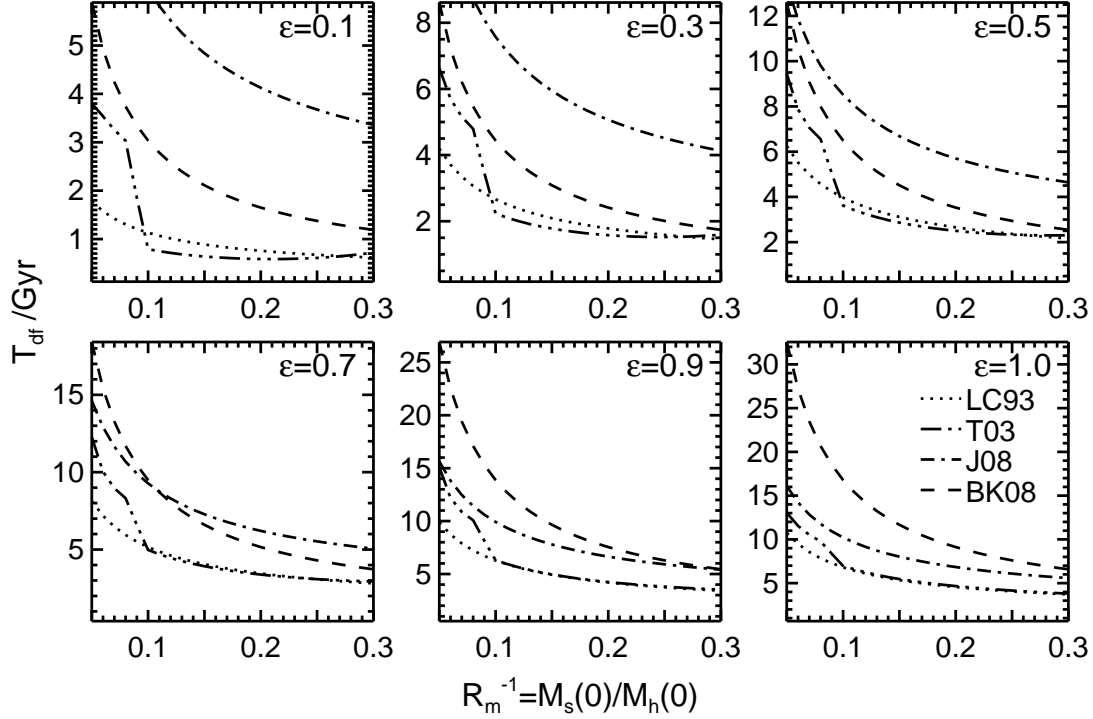


Fig. 1 Dynamical friction timescale of sinking satellite predicted by the formulas of Lacey & Cole (1993, LC93), Taffoni et al. (2003, T03), Boylan-Kolchin et al. (2008, BK08) and Jiang et al. (2008, J08). The six panels show the dependence on the orbital circularity ε , and each panel shows the dependence on the initial mass ratio between the satellite and host halo. In the results of LC93, we adopt $\ln \Lambda = \ln(1 + R_m)$, as used by T03, BK08 and J08. $\eta = 1.0$ is used in all cases.

Note that in the above two equations, the satellite is treated as a rigid object without mass loss.

With help of N-body simulation, C99 derived T_{df} for a live satellite as

$$T_{\text{df,C99}} = 1.2\varepsilon^{0.4} \frac{R_m}{f_m \ln \Lambda} \eta^2 \tau_{\text{dyn}}, \quad (3)$$

where f_m refers to the remaining fraction of satellite mass due to tidal stripping. Note that C99 only considers minor mergers. It's difficult to use this formula as the T_{df} depends on the presumed value for f_m .

Using a semi-analytical model, T03 derived their fitting formulas for T_{df} , and they were updated by Monaco et al. (2007). Their model have incorporated the effect of tides, but they ignore this effect for the large satellite (with mass $R_m^{-1} > 0.1$). Here we omit the complex formula of T03.

Using smoothed-particles hydrodynamical simulation with gas cooling and star formation in a cosmological context, J08 fitted their results with T_{df} as:

$$T_{\text{df,J08}} = \frac{0.9\varepsilon^{0.47} + 0.6}{0.855} \frac{R_m}{\ln(1 + R_m)} \sqrt{\eta} \tau_{\text{dyn}}. \quad (4)$$

BK08 considered controlled N-body simulations for two halo mergers. They gave the fitting formula of T_{df} as

$$T_{\text{df,BK08}} = 0.216e^{1.9\varepsilon} \frac{R_{\text{m}}^{1.3}}{\ln(1 + R_{\text{m}})} \eta \tau_{\text{dyn}} . \quad (5)$$

In Figure 1 we show the T_{df} as function of satellite mass and orbital circularity² predicted by LC93, T03, J08 and BK08. For a full comparison with other results, we choose $\ln \Lambda = \ln(1 + R_{\text{m}})$ in the formula of LC93. It can be seen that all results show a clear trend that T_{df} decreases with the increasing satellite mass, and increases with the orbital angular momentum and energy. However, the discrepancies among different studies are still remarkable. For example, the results of BK08 and J08 are longer than that of T03 and LC93. T03 agrees well with LC93 for large satellite ($R_{\text{m}}^{-1} > 0.1$), but disagrees for small satellite. The results of BK08 exhibits a steeper dependence on ε than other results.

3 MODELLING THE SINKING SATELLITE

This section describes the dynamical evolution of satellite based on the model of Taylor & Babul (2001); Zentner & Bullock (2003). In section 3.1 we introduce the model for the mass distribution of dark matter halo. Then we describe the physical processes governing the orbital and mass evolution of satellite. These process can be independently implemented into the model, which allows us to investigate the effect of any specific process by tune its free parameter.

3.1 Halo Properties

The dark matter halo is a gravitational self-bound system. We express the size of halo in terms of its virial mass M_{vir} and virial radius R_{vir} , which is defined as the radius within which the mean mass density of the halo is 200 times the critical density (ρ_c) of the universe at $z = 0$ (e.g., Mo et al., 1998). The Hubble constant is adopted to be $H_0 = 100h \text{ km s}^{-1} \text{ Mpc}^{-1}$ with $h = 0.7$ (BK08). The dynamical timescale can be described as

$$\tau_{\text{dyn}} = \frac{R_{\text{vir}}}{V_{\text{vir}}} = \left(\frac{R_{\text{vir}}^3}{GM_{\text{vir}}} \right)^{1/2} = 0.1 H_0^{-1} \simeq 1.40 \text{ Gyr} , \quad (6)$$

where V_{vir} is the virial velocity of a halo.

For simplicity, the dark matter halo is usually treated as a spherically symmetric system, and a simple formalism for the halo density profile is the profile of singular isothermal sphere (hereafter, ISO profile), which can be described by (e.g., Mo et al., 1998)

$$\rho(r) = \frac{V_{\text{vir}}^2}{4\pi G r^2} , \quad (7)$$

and

$$M(< r) = \frac{V_{\text{vir}}^2}{G} r . \quad (8)$$

As measured by N-body simulations, the halo density profile can be well described by the NFW profile (Navarro et al. 1997):

$$\rho(r) = \frac{\delta_0 \rho_c}{(r/r_s)(1 + r/r_s)^2} , \quad (9)$$

with r_s the scale radius, and δ_0 the characteristic overdensity. From the definition of virial radius, we can find the characteristic overdensity that $\delta_0 = 200c^3/[3g(c)]$, where $c = R_{\text{vir}}/r_s$ is the halo concentration parameter, and $g(x) = \ln(1 + x) - x/(1 + x)$. For the NFW profile, the halo mass enclosed a radius r is

$$M(< r) = M_{\text{vir}} \frac{g(r/r_s)}{g(c)} . \quad (10)$$

² Throughout this paper, we keep the orbital energy fixed as $\eta = 1.0$ to reduce the free model parameters.

The halo concentration is tightly correlated to its mass, and we use the median relation of $c \sim M$ as measured by Neto et al. (2007):

$$c(M) = 4.67 \left[\frac{M}{10^{14} h^{-1} M_{\odot}} \right]^{-0.11}. \quad (11)$$

Note that there are still debates existing in the inner shape of the NFW profile (e.g., Fukushige & Makino, 2001; Navarro et al., 2004; Stoehr, 2006; Springel et al., 2008). Varying the shape of NFW profile or using other halo profiles [e.g., ISO profile; Hernquist profile (Hernquist, 1990)] may derive a different T_{df} . However, the simulation of BK08 indicated that using a different halo profile had a change in T_{df} of only 5% (see BK08 for more details).

Except for Section 4.1 where the ISO profile is adopted to compare the model predictions with the analytical results of LC93, we use the NFW profile in other studies of this paper. When the tidal effects are considered, the satellite halo has a NFW profile at the time of entering ($t = 0$), and this profile is subsequently modified due to tidal heating, as described in Section 3.4.

In our studies, we select the host halo mass as $10^{12} M_{\odot}$, which is the typical mass used to derive the T_{df} (BK08, J08, C99). We have also tested that the predicted T_{df} has a negligible effect on the host halo mass once the mass ratio R_{m} is fixed.

3.2 Dynamical Friction

The satellite will sink into the halo center by the dynamical friction force which is caused by the gravitational interaction between the satellite and the background ‘field’ particles that make up the host halo (for a complete description, see BT87). This effect was first discussed by Chandrasekhar (1943), and the force generated by the field particles is known as the Chandrasekhar dynamical friction. By assuming that the field particles follow a locally Maxwellian velocity distribution, BT87 gave the formula of dynamical friction as

$$\mathbf{F}_{\text{df}} = -4\pi G^2 M_s^2 \ln \Lambda \rho(r) \left[\text{erf}(X) - \frac{2X}{\sqrt{\pi}} e^{-X^2} \right] \frac{\mathbf{v}_{\text{orb}}}{v_{\text{orb}}^3}, \quad (12)$$

where v_{orb} is the orbital velocity of the satellite, and $X = v_{\text{orb}}/[\sqrt{2}\sigma(r)]$ with $\sigma(r)$ the local, one-dimensional velocity dispersion of the host halo at radius r , which can be solved from the Jeans equation (BT87, Cole & Lacey, 1996). For ISO profile, $\sigma(r) \equiv V_{\text{vir}}/\sqrt{2}$; for NFW profile, we use the fitting formula of $\sigma(r)$ from Zentner & Bullock (2003). We choose the Coulomb logarithm $\ln \Lambda = \ln(1 + R_{\text{m}})$, as used by T03, J08 and BK08.

The Equation (12) was derived with the idealized assumption that the velocity distribution of the dark matter particles is Maxwellian and isotropic. Although there are debates on whether this assumption is reasonable (e.g., Manrique et al., 2003; Williams et al., 2004; Salvador-Solé et al., 2005; Bellovary et al., 2008), in this paper, we follow most authors (e.g., LC93; C99; T03; Zentener & Bullock 2003; Fellhauer & Lin 2007; BK08) to adopt the Maxwellian and isotropic velocity distribution. There are also simulations showing that this assumption is a good approximation (e.g., Cole & Lacey, 1996; Sheth, 1996; Seto & Yokoyama, 1998; Kang et al., 2002; Hayashi et al., 2003).

3.3 Tidal Mass Stripping

For a live satellite, the tidal force from the host halo will strip its mass. The tidal radius, r_t , is the distance from the center of satellite to the radius where the external differential force from the host halo exceeds the binding force of the satellite. The tidal radius can be simply solved from the following equation (von Hoerner, 1957; King, 1962; Taylor & Babul, 2001):

$$r_t^3 = \frac{GM_s(< r_t)}{\omega^2 + G[2M_h(< r)/r^3 - 4\pi\rho_h(r)]}, \quad (13)$$

with ω the angular speed of the satellite and $\rho_h(r)$ the density profile of the host halo. The mass outside r_t becomes unbound and is stripped gradually. Taylor & Babul (2001) suggested the unbound mass to be stripped at the rate that

$$\frac{dM_s}{dt} = -\frac{M_s(> r_t)}{T_{orb}}, \quad (14)$$

with T_{orb} the instantaneous orbital period (i.e., $T_{orb} = 2\pi/\omega$), which is assumed as the mass stripping timescale.

There are some uncertainties in the above mechanisms of mass stripping. (i) The tidal radius cannot be characterized by a single radius, as the zero-velocity surface (the surface defined by the tidal radius, see BT87) is not spherical. (ii) The perturbation of particles within the satellite may lead to the scatter in ω , and the zero-velocity surface is actually a shell of ‘non-zero’ thickness, while this effect is ignored in Equation (13). So the solution of Equation (13) is only an approximation for the tidal radius. (iii) The stripped mass from a satellite still remain in the vicinity of the satellite, and the interaction between the stripped and unstripped mass will perturb the satellite orbits and affect the mass loss (e.g., Fellhauer & Lin, 2007).

Owing to these uncertainties, numerical simulations have debated on how fast the unbound mass is stripped from the satellite. Zentner et al. (2005) and Diemand et al. (2007) found a stripping timescale 3.5 and 6 times shorter than T_{orb} , respectively. It was also pointed out that the stripping timescale is dependent on the satellite internal structures (Kazantzidis et al., 2004; Kampakoglou & Benson, 2007). In general, the mass loss rate can be described using a free parameter α as:

$$\frac{dM_s}{dt} = -\alpha \frac{M_s(> r_t)}{T_{orb}}, \quad (15)$$

where α describes the efficiency of tidal stripping. In Section 4.2 we will show how the T_{df} depends on α .

3.4 Tidal Heating

During the pericentric passage of satellite orbits, the gravitational field changes rapidly, and this induces a gravitational shock that can add energy to the satellite (e.g., Gnedin & Ostriker, 1997, 1999). This effect is called the tidal heating. It has been found from N -body simulations (e.g., Hayashi et al., 2003; Kravtsov et al., 2004) that tidal heating will expand the satellite and reduce its inner mass profile. Hayashi et al. (2003) introduced a modified NFW profile to describe the density distribution of a tidally heated satellite according to

$$\rho(r) = \frac{f_t}{1 + (r/r_{te})^3} \rho_{NFW}(r), \quad (16)$$

where

$$\lg f_t = -0.007 + 0.35x_m + 0.39x_m^2 + 0.23x_m^3, \quad (17)$$

and

$$\lg \frac{r_{te}}{r_s} = 1.02 + 1.38x_m + 0.37x_m^2. \quad (18)$$

In Equation (16), $\rho_{NFW}(r)$ is the original NFW density profile of the satellite at the time of entering ($t = 0$), f_t describes the reduction in the central density of the satellite, and r_{te} is the ‘effective’ tidal radius that describes the outer cutoff imposed by the tides. In Equation (17) and (18), $x_m = \lg[M_s(t)/M_s(0)]$ is the logarithm of the remaining fraction of satellite mass, and r_s is the scale radius of the satellite with NFW profile at $t = 0$. As shown by Hayashi et al. (2003), f_t and r_{te} are well fitted by the function of x_m . Both f_t and r_{te} decrease with time while a satellite is losing mass.

3.5 Orbital Evolution

Here we present explicitly the equations to solve the orbit $[\mathbf{x}(r, \theta)]$ of the satellite under gravity and the dynamical friction. The equation of motion for the satellite is given by

$$\frac{d^2 \mathbf{x}}{dt^2} = -\frac{GM_h(< r)}{r^3} \mathbf{r} + \frac{\mathbf{F}_{df}}{M_s} \quad (19)$$

with $M_h(< r)$ the mass of the host halo inside of radius r , and \mathbf{F}_{df} the dynamical friction force given by Equation (12). The orbital energy and angular momentum of the satellite will decay due to the dynamical friction as it is always opposite to the direction of motion. We define satellite to be merged with host center when it loses all its angular momentum, and T_{df} is the time interval between accretion and merger³ (as used also by BK08). The equation of motion and Equation (15) are solved using the fifth-order Cash-Karp Runge-Kutta method, in which an adaptive step-size control is embedded.

4 RESULTS

4.1 Examination on a Rigid Satellite

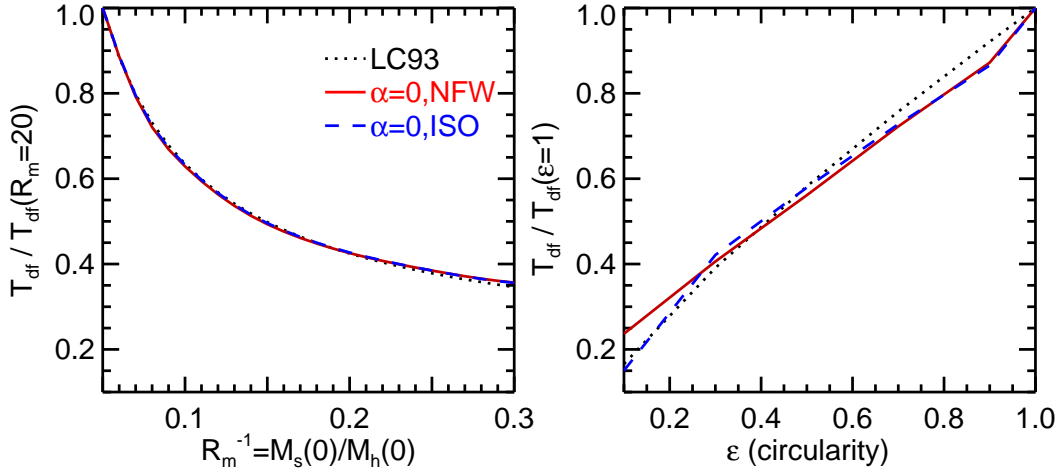


Fig. 2 The dependence of T_{df} on satellite mass (left panel) and orbital circularity (right panel) for a rigid satellite, where T_{df} is normalized to its value when $R_m = 20$ and $\epsilon = 1$, respectively. The model with $\alpha = 0$ means that a rigid satellite is considered. The results in red solid lines are computed with NFW profile, while the blue dashed lines show the results with ISO profile. Both model predictions match well with LC93's (black dotted).

Firstly we validate our model by comparing the predicted T_{df} with the LC93 result for a rigid satellite. LC93 derived T_{df} using Equation (12) and ISO profile for the host halo. In our model, we simply set $\alpha = 0$ to ‘close’ the tidal stripping and tidal heating effect, and we model the host halo with both NFW profile and ISO profile.

In Figure 2 we show the T_{df} as a function of R_m^{-1} and ϵ for a rigid satellite, with T_{df} normalized to its value when $R_m = 20$ and $\epsilon = 1$, respectively. As indicated, our results in NFW (red solid) and ISO (blue dashed) model both have the same dependences as predicted by LC93. On the other hand, the

³ Some (e.g., Kravtsov et al., 2004; Zentner et al., 2005) define satellite to be merged with the host halo when its distance to the host center is less than a fiducial radius. We find that different definitions have no significant effects.

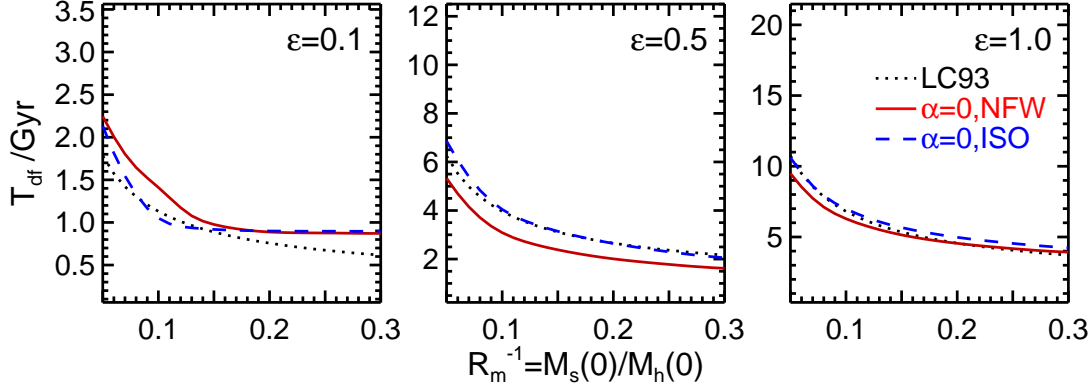


Fig. 3 Comparison of T_{df} between our model ($\alpha = 0$) and LC93 (dotted) for a rigid satellite. The T_{df} with NFW profile (red solid) and ISO profile (blue dashed) both agree well with LC93’s prediction, and they agree for all orbital circularity, although only ε with 0.1, 0.5, 1.0 are given here.

amplitudes of T_{df} from the models also agree well with the results of LC93, which is demonstrated in Figure 3. The difference resulted by varying halo profile are small and negligible, which is also concluded by BK08.

4.2 Dependence on Tidal Stripping Efficiency α

In this section we study the effects of tidal stripping efficiency (α). In Figure 4 we show the predicted T_{df} with different values of α . A larger value of α corresponds to a stronger tidal field or a rapid mass loss from the satellite. The results show a remarkable trend that the T_{df} is increased when the tidal field becomes stronger. The reason can be seen from Figure 5 which shows the evolution of satellite mass and specific angular momentum with dependence on α . The initial conditions are set as $R_{\text{m}} = 10$, $\varepsilon = 0.5$, and $\eta = 1.0$. The left panel shows that a stronger tidal field will induce more mass loss from the satellite, and this effect is more distinct at the beginning. As seen from Equation (12), the amplitude of dynamical friction has a strong dependence on the mass of satellite ($F_{\text{df}} \propto M_s^2$). So a stronger tidal stripping will lead to a slower decay of satellite angular momentum and result in a longer dynamical friction timescale, as shown in the right panel of Figure 5.

As shown in Figure 1, the predicted T_{df} from the previous results disagree with each other quantitatively. We believe that the main discrepancy is resulted in the treatment of tidal stripping, and we discuss it in more details in the following.

- T03 ignored the tidal effects for massive satellite (with mass $R_{\text{m}}^{-1} > 0.1$), and so their T_{df} are consistent with LC93’s. But T03 predicted a longer T_{df} for low-mass satellite which suffers from tidal stripping.
- The T_{df} inferred by J08 and BK08 are longer than that of T03. This is because T03 adopted a tidal stripping efficiency that is different from those in N-body simulations. T03 also used Equation (15) to describe the mass loss, but with $\alpha = 1.0$ which is too low. As shown by Zentner et al. (2005), a higher value that $\alpha = 3.5$ is required to better fit the satellite mass function from simulations (also see Gan et al., 2010). A higher value of α is also favored from Figure 6 where we compare the evolution of satellite specific angular momentum from our model (solid lines) with the simulation results of BK08 (dashed lines). We find that $\alpha = 2$ can better match the simulation results. Thus the lower value of α used by T03 explains why they obtained a lower T_{df} .

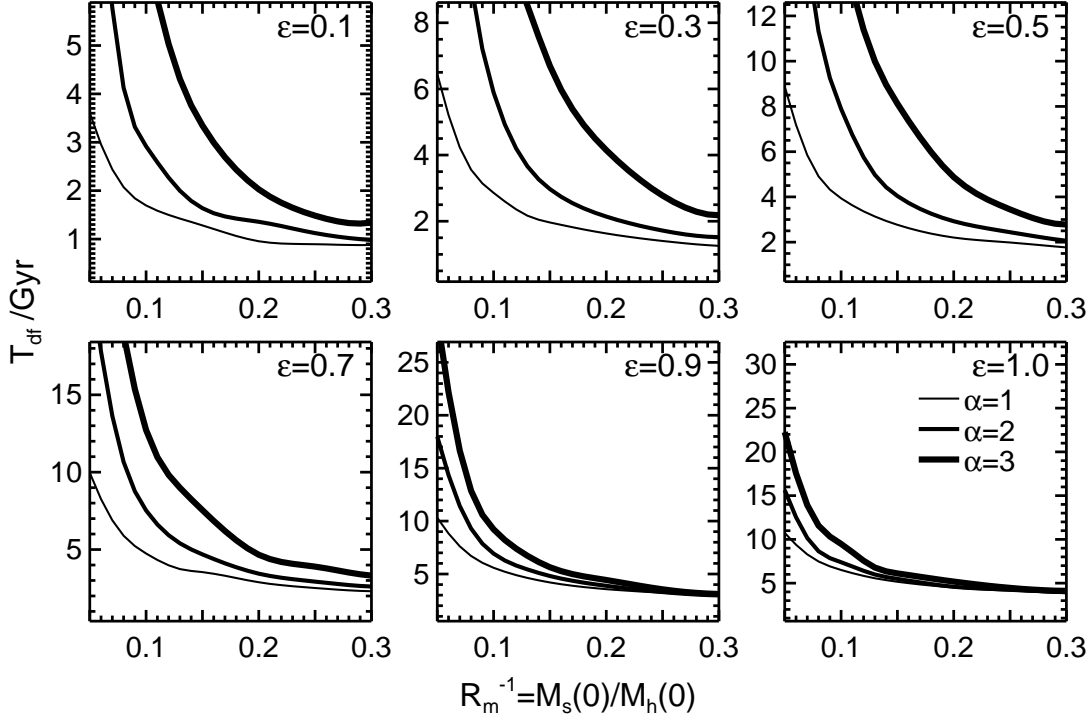


Fig. 4 The dynamical friction timescale (T_{df}) predicted by our model. The lines with increasing thickness show the effects of tidal stripping efficiency ($\alpha = 1, 2, 3$). The T_{df} is a strong function of α .

- The T_{df} of J08 is longer than that of BK08 for eccentric orbit (i.e., low ϵ)⁴. The simulation of J08 includes the process of gas cooling and star formation. The halo of a satellite is expected to contract in response to the cooling of gas (e.g., Gnedin et al., 2004; Abadi et al., 2010). During the pericentric passage, the satellite with halo contraction is resistant to the strong tidal field, and will survive for a longer time (e.g., Weinberg et al., 2008; Dolag et al., 2009). Instead BK08 performs a higher resolution simulation, in which the satellite can avoid the artificial mass loss due to the numerical effects. So the satellite will deposit more mass in the eccentric orbit and suffer stronger dynamical friction.

4.3 Dependence on Orbital Circularity ϵ

The previous results showed similar dependence of T_{df} on the initial satellite mass, but very different dependences on the orbital circularity [Equations (2)-(5)]. For example, BK08 found an exponential dependence of T_{df} on the orbital circularity, while others found a power-law dependence. Here we investigate this problem using our model with $\alpha = 1$. We compute the T_{df} as a function of ϵ for a minor merger ($R_{\text{m}}^{-1} = 0.05$) and a major merger ($R_{\text{m}}^{-1} = 0.3$), as shown in Figure 7. We find the dependence for the minor merger can be fitted to a power law, $T_{\text{df}} \propto \epsilon^{0.4}$, as predicted by C99 (long-dashed). For the major merger, the dependence is close to the result of BK08, who found the exponential law that $T_{\text{df}} \propto \exp(1.9\epsilon)$. It is not a surprise as C99 only considers minor mergers while BK08 has more samples

⁴ The results of BK08 and J08 also differ for small satellite with large ϵ , of which the T_{df} , however, are extrapolated by their formulas and exceed the Hubble time.

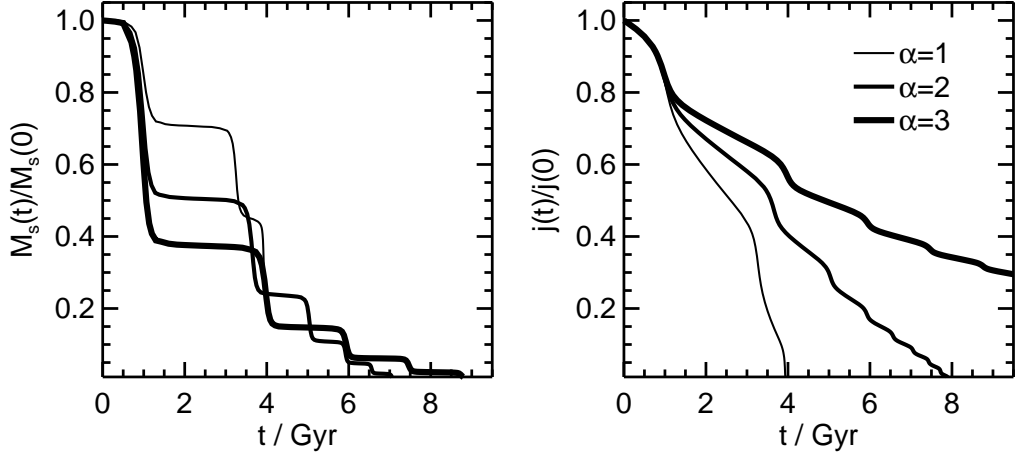


Fig. 5 The evolution of satellite mass and specific angular momentum (both are normalized to their initial value) as function of tidal stripping efficiency α . The initial conditions are that $R_m = 10$, $\varepsilon = 0.5$, $\eta = 1.0$. Strong tidal effects reduce the amplitude of dynamical friction and decelerate the loss of angular momentum.

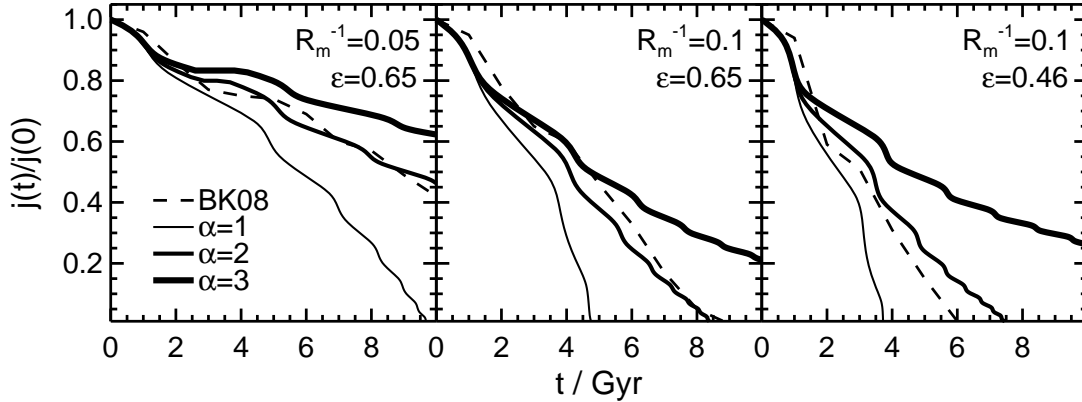


Fig. 6 Comparison of the evolution of satellite specific angular momentum between our model and BK08, with three cases of initial masses and orbits as indicated. The solid lines with increasing thickness are the model results with $\alpha = 1, 2, 3$, while the dashed line is the result from Figure 1 of BK08. The tidal stripping efficiency in the simulation of BK08 should be stronger than that in a model with $\alpha = 1$.

for the major mergers. Thus we argue that the dependence on orbital circularity is mainly determined by the distribution of mass ratio between the satellite and host halo.

5 CONCLUSION AND DISCUSSION

In this paper, we study the dynamical friction timescale (T_{df}) of a sinking satellite into a host halo. Previous results using analytical models or simulations generally agree that the T_{df} is correlated with

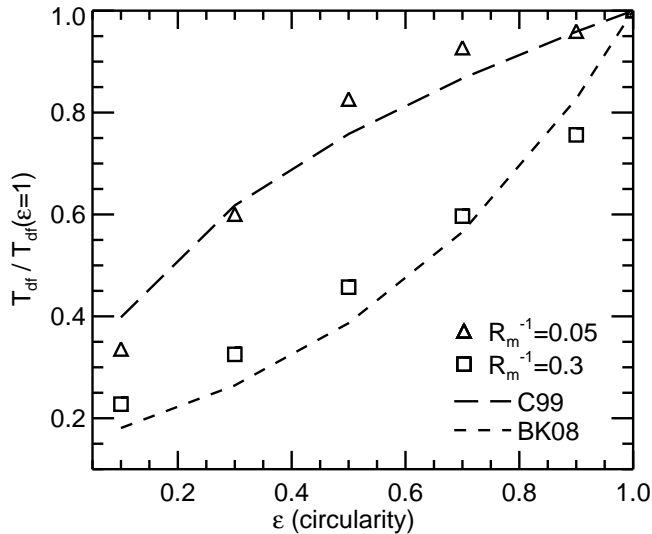


Fig. 7 The dependence of T_{df} on orbital circularity for a live satellite ($\alpha = 1$). For a minor merger (triangle), with $R_m^{-1} = 0.05$, the result shows a power-law dependence, which is similar to that of C99 (long-dashed), while for a major merger (square), with $R_m^{-1} = 0.3$, it indicates an exponential dependence, which is close to that of BK08 (short-dashed).

the mass, orbital circularity and energy of the satellite, but disagree on the amplitude of T_{df} and the dependence of T_{df} on orbital circularity. It was unclear what contributes to these discrepancies among different studies.

Aiming at interpreting these different dependences, we use a semi-analytical model similar to that of Taylor & Babul (2001) and Zentner & Bullock (2003) to derive the T_{df} . Our model considers the main physical processes governing the evolution of satellite: dynamical friction, tidal stripping, tidal heating and merger. All these process are independently described by free parameters, and it allows us to investigate the dependence of T_{df} on any process.

Firstly, we apply our model to a rigid satellite by ‘turning off’ the tidal stripping and tidal heating (i.e., $\alpha = 0$). The model predictions agree well with the LC93’s result on the amplitude of T_{df} and its dependences on satellite mass and orbital circularity. Then we study the dependence of T_{df} on the tidal stripping efficiency. We find that the T_{df} depends strongly on α , with the trend that the T_{df} increases with increasing α . A higher α leads to rapid loss of mass from satellite, than decreases the dynamical friction force. Thus this results in a slower decay of angular momentum and a longer T_{df} . We believe that the main reason for the diversity of previous result is the treatment of tidal stripping.

We also study the dependence of T_{df} on the orbital circularity (ϵ). We find that for low mass-ratio mergers ($M_s/M_h < 0.1$), T_{df} is a power law of orbital circularity. While for massive mergers ($M_s/M_h > 0.1$), the dependence of T_{df} on orbital circularity is exponential. Thus we argue that the dependence on ϵ obtained by different studies is determined by their samples, in which the mass ratio between satellite and host halo is crucial.

In this paper, we do not model the effects of baryon, as it is difficult to include the physical processes governing galaxy formation, and it is still not clear how dark matter halo will respond to the baryon at the host halo center.

The major effect of baryon is to modify the density profile of dark matter halo. There are still debates about how the baryon will change the central concentration of halo. Some found that central density increases (e.g., Blumenthal et al., 1986; Gnedin et al., 2004), but some disagreed with it. Gnedin et al. (2004) found that the halo will become more concentrated as baryons condense in the radiative cooling,

and the contraction of halo is dependent on the amount of baryon. While Abadi et al. (2010) found that the response of halo contraction depends not only on how much baryon mass has been deposited by the halo, but also on the mode of its deposition (also see Tissera et al., 2010). They showed that strong feedback by supernovae can significantly decrease the central density of halo (also see Pedrosa et al., 2009; Governato et al., 2010). The variation of T_{df} is about 20% when c_{sat}/c_{host} changes between 1 and 2 (T03; BK08).

There are also some studies showing that the dark matter haloes have constant density cores (e.g., Gilmore et al., 2007; de Blok et al., 2008; Kuzio de Naray et al., 2009; Gebhardt & Thomas, 2009; Hernandez & Lee, 2010), which can significantly suppress the effect of dynamical friction (e.g., Sánchez-Salcedo et al., 2006; Inoue, 2009). However, the typical size of the constant density core in the dark matter halo is usually less than 1 kpc (e.g., de Blok et al., 2008). The effect of the constant density core may be remarkable for the evolution of globular clusters in a dwarf galaxy (e.g., Sánchez-Salcedo et al., 2006), but not for the evolution of satellite halo in a Milky-Way sized halo.

Acknowledgements This work is funded by the National Natural Science Foundation of China No. 10573028, the Key Project No. 10833005, the Group Innovation Project No. 10821302, and by 973 program No. 2007CB815402. XK is supported by the *One Hundred Talents* project of the Chinese Academy of Sciences and by the *foundation for the author of CAS excellent doctoral dissertation*. We thank the referee for constructive comments which significantly improve our paper.

References

- Abadi, M. G., Navarro, J. F., Fardal, M., Babul, A., & Steinmetz, M. 2010, MNRAS, 847
- Bellovary, J. M., Dalcanton, J. J., Babul, A., Quinn, T. R., Maas, R. W., Austin, C. G., Williams, L. L. R., & Barnes, E. I. 2008, ApJ, 685, 739
- Benson, A. J., Lacey, C. G., Baugh, C. M., Cole, S., & Frenk, C. S. 2002, MNRAS, 333, 156
- Benson, A. J., Lacey, C. G., Frenk, C. S., Baugh, C. M., & Cole, S. 2004, MNRAS, 351, 1215
- Binney, J., & Tremaine, S. 1987, Princeton, NJ, Princeton University Press, 1987, 747 p. (BT87)
- Blumenthal, G. R., Faber, S. M., Flores, R., & Primack, J. R. 1986, ApJ, 301, 27
- Boylan-Kolchin, M., Ma, C.-P., & Quataert, E. 2008, MNRAS, 383, 93 (BK08)
- Chandrasekhar, S. 1943, ApJ, 97, 255
- Cole, S., & Lacey, C. 1996, MNRAS, 281, 716
- Cole, S., Lacey, C. G., Baugh, C. M., & Frenk, C. S. 2000, MNRAS, 319, 168
- Colpi, M., Mayer, L., & Governato, F. 1999, ApJ, 525, 720 (C99)
- de Blok, W. J. G., Walter, F., Brinks, E., Trachternach, C., Oh, S.-H., & Kennicutt, R. C. 2008, AJ, 136, 2648
- Diemand, J., Kuhlen, M., & Madau, P. 2007, ApJ, 667, 859
- Dolag, K., Borgani, S., Murante, G., & Springel, V. 2009, MNRAS, 399, 497
- Fellhauer, M., & Lin, D. N. C. 2007, MNRAS, 375, 604
- Fukushige, T., & Makino, J. 2001, ApJ, 557, 533
- Gan, J., Kang, X., van den Bosch, F. C., & Hou, J. 2010, arXiv:1007.0023
- Gebhardt, K., & Thomas, J. 2009, ApJ, 700, 1690
- Gilmore, G., Wilkinson, M. I., Wyse, R. F. G., Kley, J. T., Koch, A., Evans, N. W., & Grebel, E. K. 2007, ApJ, 663, 948
- Gnedin, O. Y., & Ostriker, J. P. 1997, ApJ, 474, 223
- Gnedin, O. Y., & Ostriker, J. P. 1999, ApJ, 513, 626
- Gnedin, O. Y., Kravtsov, A. V., Klypin, A. A., & Nagai, D. 2004, ApJ, 616, 16
- Governato, F., et al. 2010, Nature, 463, 203
- Hayashi, E., Navarro, J. F., Taylor, J. E., Stadel, J., & Quinn, T. 2003, ApJ, 584, 541
- Hernandez, X., & Lee, W. H. 2010, MNRAS, 404, L6
- Hernquist, L. 1990, ApJ, 356, 359

- Inoue, S. 2009, MNRAS, 397, 709
- Jiang, C. Y., Jing, Y. P., Faltenbacher, A., Lin, W. P., & Li, C. 2008, ApJ, 675, 1095 (J08)
- Kampakoglou, M., & Benson, A. J. 2007, MNRAS, 374, 775
- Kang, X., Jing, Y. P., Mo, H. J., Börner, G. 2002, MNRAS, 336, 892
- Kang, X., Jing, Y. P., Mo, H. J., Börner, G. 2005, ApJ, 631, 21
- Kauffmann, G., Colberg, J. M., Diaferio, A., & White, S. D. M. 1999, MNRAS, 303, 188
- Kazantzidis, S., Mayer, L., Mastroiello, C., Diemand, J., Stadel, J., & Moore, B. 2004, ApJ, 608, 663
- Kazantzidis, S., Bullock, J. S., Zentner, A. R., Kravtsov, A. V., & Moustakas, L. A. 2008, ApJ, 688, 254
- King, I. 1962, AJ, 67, 471
- Kravtsov, A. V., Gnedin, O. Y., & Klypin, A. A. 2004, ApJ, 609, 482
- Kuzio de Naray, R., McGaugh, S. S., & Mihos, J. C. 2009, ApJ, 692, 1321
- Lacey, C., & Cole, S. 1993, MNRAS, 262, 627 (LC93)
- Manrique, A., Raig, A., Salvador-Solé, E., Sanchis, T., & Solanes, J. M. 2003, ApJ, 593, 26
- Mo, H. J., Mao, S., & White, S. D. M. 1998, MNRAS, 295, 319
- Monaco, P., Fontanot, F., & Taffoni, G. 2007, MNRAS, 375, 1189
- Navarro, J. F., Frenk, C. S., & White, S. D. M. 1995, MNRAS, 275, 56
- Navarro, J. F., Frenk, C. S., & White, S. D. M. 1997, ApJ, 490, 493
- Navarro, J. F., et al. 2004, MNRAS, 349, 1039
- Neistein, E., & Weinmann, S. M. 2010, MNRAS, 405, 2717
- Neto, A. F., et al. 2007, MNRAS, 381, 1450
- Pedrosa, S., Tissera, P. B., & Scannapieco, C. 2009, MNRAS, 1877
- Salvador-Solé, E., Manrique, A., & Solanes, J. M. 2005, MNRAS, 358, 901
- Sánchez-Salcedo, F. J., Reyes-Iturbide, J., & Hernandez, X. 2006, MNRAS, 370, 1829
- Seto, N., & Yokoyama, J. 1998, ApJ, 492, 421
- Sheth, R. K. 1996, MNRAS, 279, 1310
- Somerville, R. S., & Primack, J. R. 1999, MNRAS, 310, 1087
- Springel, V., White, S. D. M., Tormen, G., & Kauffmann, G. 2001, MNRAS, 328, 726
- Springel, V., et al. 2008, MNRAS, 391, 1685
- Stoehr, F. 2006, MNRAS, 365, 147
- Taffoni, G., Mayer, L., Colpi, M., & Governato, F. 2003, MNRAS, 341, 434 (T03)
- Taylor, J. E., & Babul, A. 2001, ApJ, 559, 716
- Tissera, P. B., White, S. D. M., Pedrosa, S., & Scannapieco, C. 2010, MNRAS, 786
- von Hoerner, S. 1957, ApJ, 125, 451
- Weinberg, D. H., Colombi, S., Davé, R., & Katz, N. 2008, ApJ, 678, 6
- Williams, L. L. R., Babul, A., & Dalcanton, J. J. 2004, ApJ, 604, 18
- Zentner, A. R., & Bullock, J. S. 2003, ApJ, 598, 49
- Zentner, A. R., Berlind, A. A., Bullock, J. S., Kravtsov, A. V., & Wechsler, R. H. 2005, ApJ, 624, 505